Available online at www.sciencedirect.com

ScienceDirect

Energy Procedia 45 (2014) 298 – 307

Energy Procedia

68th Conference of the Italian Thermal Machines Engineering Association, ATI2013

On the Use of Neural Networks and Statistical Tools for Nonlinear Modeling and On-Field Diagnosis of Solid Oxide Fuel Cell Stacks

M. Sorrentino[a]*, D. Marra[a], C. Pianese[a], M. Guida[b], F. Postiglione[b], K. Wang[c], A. Pohjoranta[d]

[a]*Department of Industrial Engineering, University of Salerno, via Giovanni Paolo II 132, Fisciano (Salerno) 84084, Italy*
[b]*Department of Information Engineering, Electrical Engineering and Applied Mathematics, University of Salerno, via Giovanni Paolo II 132, Fisciano (Salerno) 84084, Italy*
[c]*University of Franche-Comté, FEMTO-ST (UMR CNRS 6174), FCLAB, rue Thierry Mieg, Belfort 90000, France*
[d]*VTT-Technical Research Center of Finland, P.O.Box 1000, VTT 02044, Finland*

Abstract

The paper reports on the activities performed within the European funded project GENIUS to develop black-box models for modeling and diagnosis of solid oxide fuel cell (SOFC) stacks. Two modeling techniques were investigated, i.e. Neural Networks (NNs) and Statistical Tools (STs). The deployment of NNs was twofold: Recurrent Neural Networks (RNNs) and an NN classifier were developed to simulate transient operation of SOFCs and identify some specific faults that may occur in such devices, respectively. On the other hand, STs are based on a stepwise multiple regression.
Data for model development were obtained from experiments specifically designed to reach maximal information content. The final aim was to obtain highly general models of SOFC stacks' operation in both transient and steady state. All the developed black-box models exhibited high accuracy and reliability on both training and test data-sets. Moreover, the black-box models were also proven effective in performing real-time monitoring and degradation analysis for different SOFC stack technologies.

Selection and peer-review under responsibility of ATI NAZIONALE

Keywords: Black-box models; Solid Oxide Fuel Cells; recurrent neural network; neural network based classification; step-wise regression analysis.

* Corresponding author. Tel.: +39-089-96-4100; fax: +39-089-96-4037.
E-mail address: msorrentino@unisa.it

Selection and peer-review under responsibility of ATI NAZIONALE
doi:10.1016/j.egypro.2014.01.032

1. Introduction

In the field of system maintenance, fault diagnosis has become an issue of primary importance in modern process automation as it provides the prerequisites for the purpose of system failure prevention. A diagnostic tool conception begins usually by mathematically modeling the process of the considered entity so as to simulate its behaviors mostly without faults. Then, through a comparison between the measured parameters and the simulated ones without the presence of fault, a residual vector can be generated and evaluated to determine if a fault has happened. The residuals should be ideally close to zero under fault-free conditions, minimally sensitive to noises and disturbances, and maximally sensitive to the studied faults [1]. Once the fault is confirmed being present, a decision-making process will be performed to identify the fault type, based on a pre-constructed fault signature matrix. Sometimes, models for specific faults can also be set up to support for fault identification.

In fuel cell engineering, the application of model-based approach has been investigated for fuel cell system diagnosis. The majority of models rely on analytical approaches, mainly based on physical equations. For example, Escobet et al. [2] used this kind of fuel cell model to diagnose six faults of interest in a PEMFC system: 1) increase of the friction in the compressor motor and 2) its overheating, 3) blocking of the channels in the diffusion layer of the fuel cell, 4) leakage in the air supply manifold, 5) the compressor motor control failure and 6) the stack temperature control failure. Four fault feature variables, i.e. the oxygen excess ratio, the compressor's current density and its speed as well as the stack voltage, were used to characterize these faults. The sensitivity of the residual to a fault was studied in order to differentiate the faults. A theoretical relative fault sensitivity matrix with the residual sensitivity in the row and the faults in columns was derived as a reference to support for fault identification. The fundamental difficulty related to the physical-model-based diagnosis is the fact that there are always modeling uncertainties due to un-modeled disturbances, simplifications, idealizations, linearization, model parameter inaccuracies and so on, which restrict model generalizability. Moreover, conventional analytical model can only serve for linear systems, whereas a fuel cell system a complex, non-linear system.

By contrast, black-box model is more suitable for FC system diagnosis. Such models do not apply explicit physical equations but are based on artificial intelligence technology, which is used to learn system's input-output relationship from the measured database [3]. They are adaptive for dynamic systems. In the research of Steiner et al. [4], a neural network model was built and trained/parameterized with experimental data to estimate the cathode pressure drop, the dew point temperature, the stack temperature and the air inlet flow rate of a PEMFC stack, with the aim of diagnosing flooding phenomenon in the fuel cells. Then, the model was developed to estimate another feature variable, i.e. the stack output voltage, for diagnosing both flooding and drying failures in the PEMFC [5].

This paper presents three different implementations of black-box models for describing SOFC stacks performance. The discussed models and their use are as follows: i) Recurrent neural network (RNN) model for dynamic modeling of the SOFC stack voltage; ii) Static neural network (NN) model for identifying specific faults in an SOFC power system; iii) Stochastic models (SMs) for determining the most effective correlations among stack performance and operating variables. These models were designed for the embedding in a model-based algorithm for SOFC diagnosis [6].

As for RNN-related activities, three separate RNNs were developed, related to the transient experimental tests provided by Topsoe, VTT and Wärtsilä, respectively. The RNNs developed on Topsoe and VTT transients were trained and tested on data-sets 1 and 4, respectively (see Table 1). Specific transient experiments were provided by Wärtsilä to UNISA to develop an RNN already suitable for subsequent implementation as real time monitoring software (i.e. data-sets 5 and 6 in Table 1). Subsequently, a preliminary application of RNNs both for monitoring and diagnostics purposes is presented.

The NN classifier, developed referring to the experimental data acquired within the RealSOFC project (i.e. data-set 7 in Table 1), was used to train an NN that serves as a classifier to identify the fault type. This model can make a relatively high accuracy of estimation for two specific faults, as discussed in the following sections.

Finally, some empirical (stochastic) models have been built by using both mixed-effects models and regression-based ones. The former approach has been effectively applied to the long-term experiments represented in the Hexis RealSOFC preliminary data (see data-set 7 in Table 1) in order to describe the intrinsic variability of SOFC cells composing a stack. The latter has been developed to characterize the stack output voltage as a function of four parameters in (quasi) steady-state conditions and to highlight the most relevant parameters for the description of the

SOFC behavior by means of stepwise approaches. It has been successfully applied to both the VTT I and Topsoe data-set (see Table 1).

2. EXPERIMENTAL DATA FOR BLACK-BOX MODEL DEVELOPMENT

To obtain sufficient data for the development and validation of the presented black-box models, several experiments on SOFC stacks and systems were carried out. The stack tests were designed to abide to the design of experiments principles, using randomization of test conditions and factorial experimenting to identify the most relevant system inputs. These tests were carried out by three different partners, at their own facilities. The data from full systems were both regular operational data as well as data from planned tests. The data series utilized in the model development are listed and described shortly in Table 1. Data-sets 1, 2 and 3 where obtained applying the Design of Experiments methodology presented in [8]. On the other hand, in order to better understand the behavior of an SOFC stack around its nominal working condition in terms of fuel (FU) and air (AU) utilization, furnace temperature (T_{furn}, °C) and current density (J, Acm^{-2}), other experimental testing conditions were analyzed in data-set 4. Particularly, in every testing point, a random value has been added to the levels of parameters to better train neural networks. Furthermore, experimental points have been explored randomly in order to reduce effects of unknown/uncontrolled variables. The experimental points are reported in Table 2, where the parameters levels have been expressed as a fraction of their nominal value. The number of tested levels is different for the parameters and it is related to the relevance of the parameter for the stack behavior. Indeed, 5 levels has been chosen for the most relevant parameter J, while 3 levels have been proposed for T_{furn} and AU, and 2 for FU. Such choices are justified by the following considerations: exploring a large current density range ensures to properly investigate the variation of main polarization losses (i.e. activation, Ohmic and polarization) as a function of current density; of course the impact played by the other operating parameters is worth to be investigated to provide the neural networks' training procedure with the most informative physical content. Therefore, three temperature levels were randomly investigated to enable black-box models to well describe the positive effect of temperature increase on polarization losses, especially at medium-high current density. Fuel and air utilization also were varied at two random levels to take into account the twofold effects played by a larger amount of either fuel or air with respect to their respective stoichiometry values: indeed, increasing fuel/air amount causes the reactant partial pressure to increase, thus having a positive effect on SOFC performance; on the other hand, higher amount of reactants leads to reduced operating temperatures, which in turn results in higher polarization losses. In this work only two random levels were selected for FU and AU (see Table 2), as they play a less significant effect on overall cell performance than operating temperature, which has a more direct impact on polarization losses.

Table 1. Summary of the data series utilized in models development.

Data-set	Data series name	Test object	Data description	Usage
1	Topsoe	Topsoe stack	DoE test data + extended holds	RNN model training and validation
2	VTT I	HTceramix stack	DoE full factorial test data	Statistical model development and validation
3	VTT II	HTceramix stack	DoE full factorial test data	RNN model validation
4	VTT III	HTceramix stack	86 random operating points	RNN model training and validation
5	Wärtsilä I	Wärtsilä multi-stack system	Long-term operating data	RNN model training and validation
6	Wärtsilä II	Wärtsilä multi-stack system	Long-term operating data	RNN model training and validation
7	Hexis [7]	Hexis single-stack system	Ad hoc system test data	Fault classifier NN development

In addition to test data that were specifically collected for the development of the models presented here, also historical test data from the EU funded project RealSOFC were used for early-phase development of the models [7].

The following sub-section provides a deeper presentation of experimental activities carried-out at VTT facilities.

2.1. VTT experimental activity

The experimental stack test set-up in the VTT laboratory is illustrated in Figure 1. In both tests, a 6-cell S-design short stack manufactured by HTceramix (Switzerland) was instrumented in an insulated furnace, with heater

elements around the stack. The gas pipelines as well as the current collectors (CCs) access the stack from the furnace bottom through tight holes.

Mass flow controllers (Bronkhorst) were utilized to control the gas components' flow and a temperature-controlled bubbling chamber was utilized to set the fuel humidity. A (Kikusui) DC load was used to draw current from the stack. The entire test apparatus was controlled and the measurement data was logged at 1 Hz via a PLC-based automation system.

Test procedures at VTT – Three series of experiments (VTT IIII) were carried out to generate the data necessary for a full factorial DoE analysis on the stack and an extended randomized stack test series. In the VTT I and II tests, a full factorial DoE test was completed. In the VTT I test, the fuel was a $H_2/N_2/H_2O$ mixture, while in VTT II (and VTT III) test the fuel contained also CH_4 and CO_2. The VTT III test series was a 86-point series of random operating points. In all tests the stack was operated galvanostatically (i.e. the stack current was set by the operator).

The examined parameters in all the experiments (i.e. system inputs) were: J, T_{furn} and FU. Also the fuel water content x_{HUM} (-) was examined during the VTT II test.

The system response was monitored by measuring 23 variables, including individual cell voltages, flow pressures, stack and flow temperatures and anode exhaust oxygen content.

Measuring each experimental data point included gradually transferring the system conditions to those given by the test matrix and letting the system stabilize in each condition for 4-5 hours, leading to a total of a 6-hour measurement period per data point. A system I-V curve (current vs. voltage curve) was measured at each data point after the stabilization period. The I-V curves enable checking that the stack operation was consistent throughout the test.

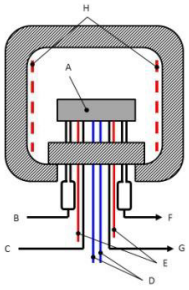

Figure 1. The test set-up. A: Stack, B: Air inlet, C: Fuel inlet, D: Anode CCs, E: Cathode CCs, F: Air outlet, G: Fuel outlet, H: Heaters.

Table 2. Parameters levels considered in the randomization conducted on Data-set 4 definition.

	Random levels				
	1	2	3	4	5
FU	1.00	0.85-0.75			
AU	1.20-1.15	1.00	0.85-0.75		
T_{furn}	1.20-1.15	1.00	0.85-0.76		
J	2.00-1.80	1.60-1.40	1.00	0.60-0.40	0.20

3. RNN MODEL DEVELOPMENT

Recurrent Neural Networks are derived from static neural networks by considering feedback connections among the neurons. Thus, a dynamic effect is introduced into the computational system by a local memory process. Moreover, by retaining the non-linear mapping features of the static networks, RNNs are suitable for black-box nonlinear dynamic modeling. For a more detailed description of the background on RNN the reader is addressed to the abundant bibliography on the topic [9, 10, 11, 12].

Figure 2(a) shows the basic RNN structure adopted hereinafter to simulate SOFC voltage as a function of main system operating variables. On the other hand, the following eq. (1) expresses the nonlinear dependence of RNN

output on current (i.e. at time t) and past information (i.e. from time t-1 to time t-m) on the values of the input variables. Eq. (1) also highlights how the dynamic effect is introduced by providing, as inputs, also information on previous simulated values of the output variables (i.e. from time t-1 to time t-n).

$$\hat{y}(t+1) = F\left[u(t),\ldots u(t-m), \hat{y}(t),\ldots,\hat{y}(t-n)\right] \quad (1)$$

When training and developing an RNN model, one of the most troublesome task is the selection of the best network structure, both in terms of past input information (see eq. (1)) and number of hidden neurons. In this work, a trial and error procedure was set-up to determine the best network structure per each available data-set (see Table 1), yielding on output the RNN topologies detailed in Table 3. It is worth remarking here that the number of past information on RNN output (see eq. 1) was kept constantly equal to n=2, since such a value was proven to be sufficiently reliable in previous RNN development works [13].

Table 3. RNN structure specifications.

RNN	Training and test data-set (see Table 1)	Past Inputs (i.e. m in eq. 1)	Hidden neurons
RNN1	Topsoe	2 for temperatures,1 for current density and flows	8
RNN2	VTT III	2 for temperatures, 1 for current density and flows	8
RNN3	Wärtsilä multi-stack system	10	5

3.1. RNN results

Figure 2(b) and Figure 3 show the experimental curves and trajectories simulated by the RNNs trained for the Topsoe (i.e. RNN1, see Table 3) and the HTceramix stack (i.e. RNN2) tested by VTT, respectively. The comparisons illustrated in Figure 2(b) and Figure 3(a) indicate that both RNN1 and RNN2 achieved quite a high accuracy level (i.e. with error safely bounded below 2%). In order to further analyze RNN generalization capabilities, RNN2 was tested on data-set 3 also (i.e. VTT II, see Table 1). The comparison between experimental and simulated trajectory, shown in Figure 3(b), indicates that still a satisfactory agreement was achieved, but with errors slightly higher than data-set 4, around 4 % on average. Nevertheless, it must be considered that the data-set used for RNN2 training was acquired as part of the same transient, from which the test-set shown in Figure 3(a) was extracted. On the other hand, data-set 3 was acquired at another time, with different operating and environmental conditions. Therefore, it can be concluded that RNN models can potentially ensure adequate accuracy throughout SOFC lifetime.

The next RNN3 was trained and initially tested against the first data-set provided by Wärtsilä. Figure 4(a) shows that the final part of data-set 5 (see Table 1) was used to train the network, while the first part was selected as first test-set. Such a choice is justified by the fact that the final part of the trajectory shown on Figure 4(a) includes a step change (particularly, a reduction) in load, which in turn results in a voltage increase, as expected from fuel cell theory [14].

The correct selection of the training-set allowed achieving satisfactory accuracy on both the first test-set (i.e. first part of the transient shown on Figure 4(a)) and the second test-set, as shown in Figure 5. The last figure actually consists of two sub-plots, one relative to the stack n. 1 and the second to stack n. 18 of the multi-stack system experimented by Wärtsilä (see Table 1). Particularly, the comparisons illustrated in Figure 5 indicate how the voltage simulated by RNN3, which corresponds to a value averaged on the different stacks the multi-stack system consists of, can be considered as a reliable estimator of global performance. On the other hand, the small offset present in the time-window [0-400] h of Figure 5(a) highlights the importance of developing one single RNN per each stack, especially when aiming at RNN-based real-time monitoring and diagnosis.

Finally, Figure 4(b) describes the intended deployment of RNNs for monitoring both stack and multi-stack performance throughout their lifetime, aiming also to diagnose the occurrence of excessive degradation. Particularly, since the RNN can be trained on sufficiently extended transients, it can easily learn the normal degradation, which SOFC stacks undergo throughout their lifetime. Therefore, if the error significantly exceeds the level indicated by

the comparisons shown on Figure 4(a) and Figure 5, as qualitatively shown on Figure 4(b), an alarm can be activated to avoid keeping operating the SOFC stack under over-severe degradation.

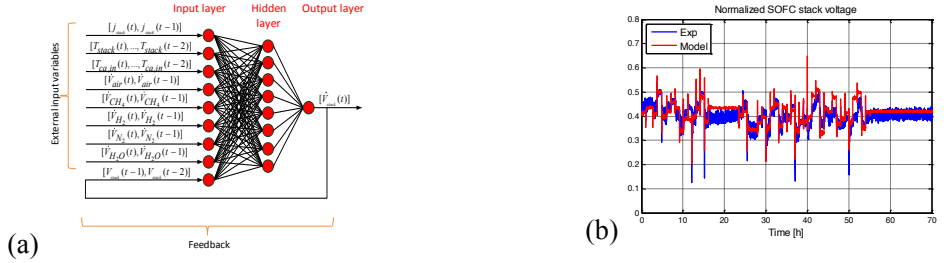

Figure 2. (a) schematic representation of an exemplary RNN estimator of SOFC voltage; (b) Comparison between measured and simulated stack voltage on the test-set extracted from data-set 1, see Table 1.

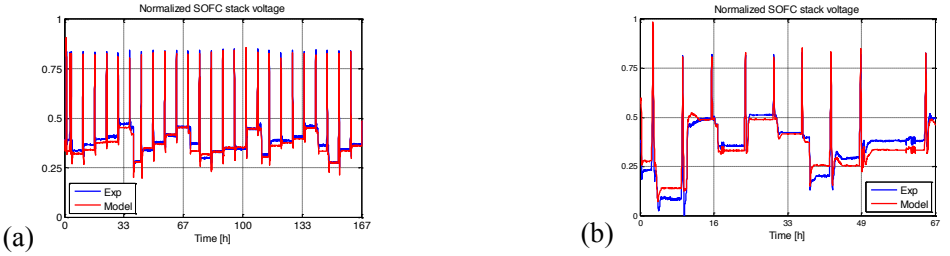

Figure 3. Comparison between measured and simulated stack voltage on the test-set extracted from data-set 4 (a) and data-set 3 (b), see Table 1.

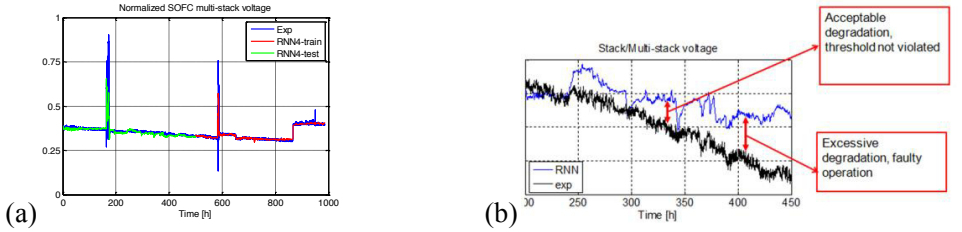

Figure 4. (a) comparison between measured and simulated stack voltage on the test-set extracted from data-set 5, see Table 1; (b) qualitative description of RNN potentialities for real time monitoring of SOFC stack/multi-stack.

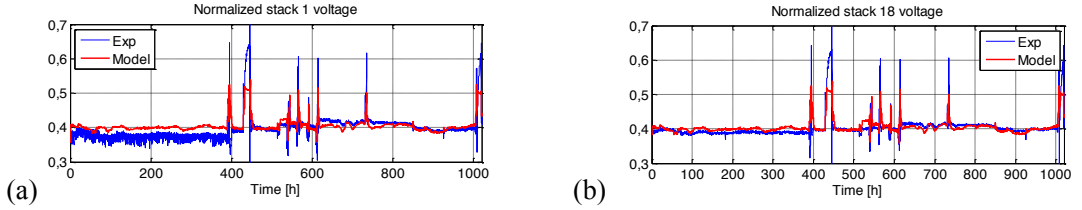

Figure 5. Comparison between measured and simulated stack voltage on data-set 6, see Table 1.

4. Statistical tools for SOFC behavior

A possible approach to model steady-state SOFC behavior can be based on the adoption of regression techniques. In particular, it can be useful to identify the most relevant factors for the cell/stack output voltage: to this aim it can

be adopted a multiple regression analysis with a stepwise approach, in order to model a measured quantity as a function of different influencing variables, such as temperatures, current density and so on.

Stepwise multiple regression introduces some automatic procedures to select the most significant regressors X (typically influencing factors and some functions involving them) for a measured quantity Y. For instance, in an experiment depending on the values of 4 factors the measured quantity Y can be modeled as a function of direct effects X_1, X_2, X_3, X_4 and their interactions as follows [15]:

$$\begin{aligned} Y = {} & Y_0 + a_1X_1 + a_2X_2 + a_3X_3 + a_4X_4 + a_{12}X_1 \cdot X_2 + a_{13}X_1 \cdot X_3 + a_{14}X_1 \cdot X_4 + a_{23}X_2 \cdot X_3 + \\ & a_{24}X_2 \cdot X_4 + a_{34}X_3 \cdot X_4 + a_{123}X_1 \cdot X_2 \cdot X_3 + a_{124}X_1 \cdot X_2 \cdot X_4 + a_{134}X_1 \cdot X_3 \cdot X_4 \\ & + a_{234}X_2 \cdot X_3 \cdot X_4 + a_{1234}X_1 \cdot X_2 \cdot X_3 \cdot X_4 \end{aligned}$$

Under the assumption of neglecting 3-order and higher interactions, it reduces to:

$$\begin{aligned} Y = {} & Y_0 + a_1X_1 + a_2X_2 + a_3X_3 + a_4X_4 + a_{12}X_1 \cdot X_2 + a_{13}X_1 \cdot X_3 + a_{14}X_1 \cdot X_4 + a_{23}X_2 \cdot X_3 + \\ & a_{24}X_2 \cdot X_4 + a_{34}X_3 \cdot X_4 \end{aligned} \quad , \tag{2}$$

where the number of parameters to be estimated from data is 11, namely Y_0 and the a_{ij} coefficients.

4.1. Application of stepwise regression methodology to GENIUS 1st test round data

In order to show the said approach the data-set 2 presented in Table 1 is analyzed, provided by VTT in the GENIUS Project [16] 1° test round during tests on the HT Ceramix stack. Henceforth, the following notation is assumed:

- Y is the voltage of every cell composing the stack (6 cells) or the stack output voltage;
- X_1 is the furnace temperature (T);
- X_2 is the current density (J);
- X_3 is the Fuel Utilization (FU);
- X_4 is a quantity related to lambda CPO (λ_{CPO}).

Data have been collected in 21 different operational points of the stack: 16 points given by a 2^4 full factorial DoE and 5 points in the center of the factors domain, where some randomization has been introduced in the experiment setup. Figure 6(a) shows the time series of the measured voltages of cells composing the stack. Since the regression analysis aims to determine a *steady-state* empirical model for the stack voltage as a function of $X_1,\ldots, X_4$, the measured quantities in every operational point have been averaged in time periods representative of steady-state conditions (in gray in Figure 6(a)).

The model of the voltage can be written in the form $\mathbf{Y} = \mathbf{X\beta} + \boldsymbol{\varepsilon}$, where $\mathbf{Y}$ is the vector of the mean values of the voltage in the operating conditions (henceforth, the observations), $\boldsymbol{\beta}$ is the vector of parameters to be estimated, such as Y_0 and the a_{ij} in (1), $\mathbf{X}$ is the matrix of regressors, also known as design matrix, and $\boldsymbol{\varepsilon}$ is the experimental noise vector. In this model, $p = 11$ parameters should be estimated from $n = 21$ observations. Indeed, the least square estimates of the said parameters can be computed by

$$\hat{\boldsymbol{\beta}} = \left(\mathbf{X}^T\mathbf{X}\right)^{-1}\mathbf{X}^T\mathbf{Y} \quad ,$$

while a confidence interval (CI) , at a given level $1 - \alpha$, can be computed for every parameter as follows:

$$\left[\hat{\beta}_i - t_{1-\frac{\alpha}{2},n-p}\hat{\sigma}\sqrt{\left(\mathbf{X}^T\mathbf{X}\right)^{-1}_{ii}}\,,\ \hat{\beta}_i + t_{1-\frac{\alpha}{2},n-p}\hat{\sigma}\sqrt{\left(\mathbf{X}^T\mathbf{X}\right)^{-1}_{ii}}\right] \quad , \tag{3}$$

where the standard deviation is computed as the square root of the variance estimated by its unbiased estimator:

$$\hat{\sigma} = \sqrt{\frac{\mathbf{Y}^T\mathbf{Y} - \hat{\boldsymbol{\beta}}^T\mathbf{X}^T\mathbf{Y}}{n-p}} \quad . \tag{4}$$

In a regression analysis, the *i*-th coefficient is statistically significant if its CI does not include 0: this approach is equivalent to a *t*-test with the null hypothesis $\hat{\beta}_i = 0$. It implies that the corresponding factor or interaction in (2) is statistically significant to model the dependant variable *Y*. On the contrary, *i*-th factor/interaction is not relevant to model the behavior of *Y*.

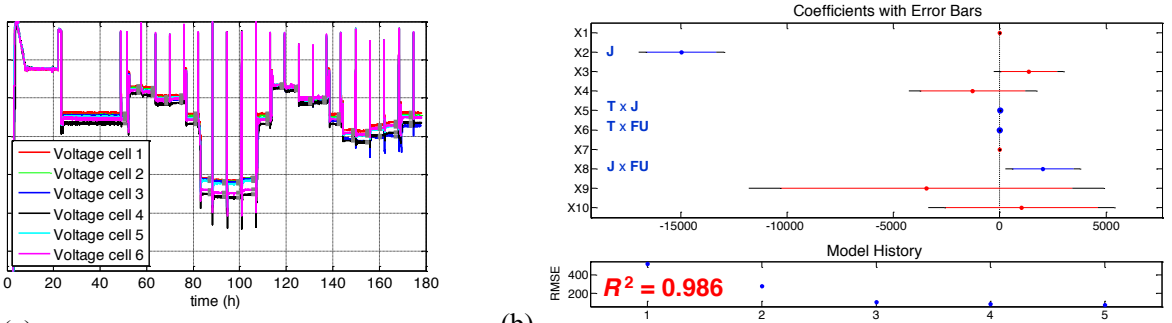

Figure 6. (a) Cell voltage time series in data-set 2 (see Table 1), reporting in gray the time periods representing steady-state conditions for the stack in the operational points; (b) a graphical output of a tool implementing the stepwise approach applied to the stack voltage from data-set 2.

By exploiting this idea, it is possible to add or remove independent variables (i.e. influencing factors) in order to select an adequate model for *Y*. In a so-called *stepwise approach* to multiple regression analysis, a sequence of *t*-tests (or *F*-tests) can be used to include or exclude single variables or some variables. When no variable can be added or removed by significantly improve the empirical model for *Y*, the procedure stops and the independent variables involved in the final model represent the most significant influencing factors for *Y*.

Therefore, the stepwise regression analysis can be adopted to model SOFC cells/stack steady-state behaviour.

In particular, it was considered the SOFC stack (output) voltage *Y*, given by the sum of cell voltages; however, it can be applied to every single cell voltage, as well. By selecting a *p*-value for entrance equal to 0.05 and an exit *p*-value equal to the same value for every independent variable, the most significant influencing factors for stack voltage are: the current density J; the interaction between J and the temperature T; the interaction between T and the fuel utilization FU; and the interaction between J and FU.

The coefficient of determination corresponding to the empirical model involving only those factors is $R^2 = 0.986$, as depicted in Figure 6(b). Besides the most relevant factors and interactions, it points out that the lambda CPO seems to have no significant influence on the stack voltage. Similar results (not shown) were obtained for single cell voltages.

5. A CLASSIFICATION MODEL BASED ON NEURAL NETWORK

In practice, the degradation of a fuel cell stack is usually attributed to improper operating conditions caused by BoP failures (such as temperature control fault, fuel leakage, air blower failure etc.). At the beginning of the operation under these faulty conditions, the performance degradation of the stack is not quite visible until considerable damage occurs inside the fuel cell. It is thus necessary to perform an early diagnosis on the fuel cell stack to examine its actual operating condition. To achieve this, an NN model can be set up to distinguish faulty operating conditions from the nominal ones, used as a classifier.

5.1. Structure of the NN model

In this work, two faulty operating conditions (OC1 & OC2) for SOFC stack were considered. OC1 makes SOFCs operate in a high temperature gradient environment, leading to mechanical damage (ex: delamination) in the fuel

cells. OC2 can result in anode re-oxidation, accelerating the degradation of SOFCs. Under each operating condition, two classes, “no degradation” and “degraded”, were defined to describe the actual state of health of the stack. Hence, there are 4 faulty operation modes to consider (see Table 4).

The NN model consists of two parallel sub-networks: one is composed of 4 perceptron networks, each of them represents one faulty operation mode (simply labeled from 1 to 4); the other is a two-layer forward neural network used to estimate the matching degree to the class. These two networks are connected in parallel and have common input. There are 12 input variables, including 7 operating variables and 5 response variables of the stack:

- Controllable operating variables:
  - Natural gas flow-input 1 (g/h);
  - Natural gas flow-input 2 (g/h);
  - CPO air flow (l/h);
  - Cathode air flow (g/h);
  - Preheating CPO (%);
  - Preheating air (%);
  - Stack current (A).
- Response variables of SOFC:
  - Temperature at bottom of stack (°C);
  - Temperature at top of stack (°C);
  - Input fuel temperature of CPO (°C);
  - Output gas temperature of CPO (°C);
  - Stack voltage (V).

The NN serves at analyzing the measurement of these inputs and gives decision on the fuel cell operation mode (see Figure 7(a)). When all of the four perceptron networks give null output, it means that the SOFC stack is operated in proper operating condition and without degradation; the fault type number is “0”. On the contrary, when the stack is operated improperly, one of the perceptron networks will generate a “1”, indicating the faulty operation mode.

This NN model (see Figure 7(b) and 7(c)) was trained with the experimental dataset from RealSOFC project, which aimed to understand the degradation mechanisms of SOFC stacks. These data were recorded on the HEXIS 5-cells (i.e. data-set 7 in Table 1) test rig at which 4 long-term (more than 6000 hours) experiments were carried out respectively on 4 stacks of the same type and manufacturing technology. Redox cycling and/or thermal cycling were simulated during some of these experiments. The redox cycles were simulated by switching off the gas and the current at constant temperature. The thermal cycles were realized by means of shutting down the system abruptly, which also caused indirect redox cycling due to the current vanishing.

5.2. Validation results

For testing the classifier, a dataset including 639 samples was used. The ratios of correct classification are given in Table 4. The network was proven quite reliable in classifying faults 1 and 2, whereas further work is required to well classify faults 3 and 4.

6. CONCLUSIONS

Three RNNs have been developed to simulate the stack voltage of two different stacks and one system, i.e. Topsoe, HTceramix and Wärtsilä, respectively.

In all cases the developed RNNs show interesting results; particularly, the ability to simulate the stack voltage makes these models suitable to be implemented into an online applicable model-based diagnosis tool. As expected from neural network theory, the accuracy of the results is strongly influenced by the possibility to use transient maneuvers covering the largest area of the input variables domain.

Furthermore, stepwise regression can be adopted to identify the most relevant parameters and their interactions for SOFC cells/stacks behavior. An empirical model has been provided for the VTT II stack voltage. This model includes only the most significant influencing factors for the output voltage, such as J and the interactions T–J, T–FU and J–FU, and suggests that lambda CPO has no significant influence. Finally, static NNs were proposed to develop a fault classifier aimed at distinguishing SOFC stack’s 4 faulty operating modes. This classifier is able to distinguish the high temperature gradient operating environment for SOFCs and discriminate the good and the degraded state of health of the SOFC stack under this operating condition.

Table 4. The accuracy of the classifier.

	Fault 1	Fault 2	Fault 3	Fault 4
Description	OC1 + No degradation	OC1 + Degraded	OC2 + No degradation	OC2 + Degraded
Accuracy	88.75%	76.88%	32.81%	56.56%

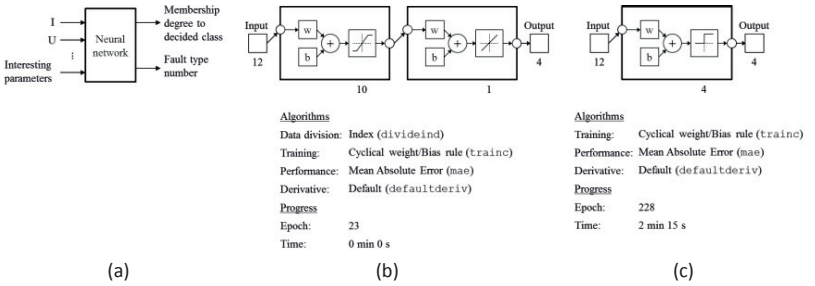

Figure 7. (a) input and output of the classifier, (b) 2-layer net. for membership degree simulation, (c) 4-outputs perceptron net. for classification.

Acknowledgements

The research leading to these results has received funding from from the European Union's Seventh Framework Programme (FP7/2007e2013) for the Fuel Cells and Hydrogen Joint Technology Initiative under grant agreement n° [245128] 10 (Project - GENIUS, GEneric diagNosis Instrument for SOFC systems)..

References

[1] Athamena B., Abbassi H.A., 2003, Fault Detection and Isolation Using Hybrid Parameter Estimation and Fuzzy Logic Residual Evaluation, Informatica, vol. 7, n°1, pp. 29-38.
[2] Escobet T., Feroldi D., de Lira S., Puig V., Quevedo J., Riera J., Serra M., 2009, Model-based fault diagnosis in PEM fuel cell systems, Journal of Power Sources, vol. 192, pp. 216-223.
[3] Wang K., Hissel D., Péra M.C., Steiner N., Marra D., Sorrentino M., Pianese C., Monteverde M., Cardone P., Saarinen J., 2011, A Review on solid oxide fuel cell models, International Journal of Hydrogen Energy, vol. 36, n°12, pp. 7212-7228.
[4] Steiner N.Y., Candusso D., Hissel D., Mocoteguy P., 2010, Model-based diagnosis for proton exchange membrane fuel cells, Mathematics and Computers in Simulation, vol. 81, pp. 158-170.
[5] Steiner Y.N., Hissel D., Moçotéguy P., Candusso D., 2011, Diagnosis of polymer electrolyte fuel cells failure modes (flooding & drying out) by neural networks modeling, International Journal of Hydrogen Energy, vol. 36, pp. 3067-3075.
[6] Arsie I., Di Filippi A., Marra D., Pianese C., Sorrentino M., Fault Tree Analysis Aimed to Design and Implement on-field Fault Detection and Isolation Schemes for SOFC Systems, ASME 2010 8th International Conference on Fuel Cell Science, Engineering and Technology, June 14–16, 2010 , Brooklyn, New York, USA, DOI: http://dx.doi.org/10.1115/FuelCell2010-33344.
[7] RealSOFC Realising Reliable, Durable, Energy Efficient & Cost Effective SOFC Systems, EU project n. 502612, Final Report, 2006.
[8] Esposito A., Postiglione F., Pohjoranta A., Wang K., Pofahl S., Mocoteguy P., Guida M., Pianese C., Hissel D., Péra M.C., Experimental Test Plan and Data Analysis Based on the Design of Experiment Methodology, Proc. ASME ESFuelCell 2012, pp. 293-302, San Diego (CA - USA), 23-26 luglio, 2012, ISBN: 978-0-7918-4482-3, DOI: 10.1115/FuelCell2012-91114.
[9] Arsie I., Pianese C., Sorrentino M., 2009, Development and real-time implementation of recurrent neural networks for AFR prediction and control, SAE International Journal of Passenger Cars - Electronic and Electrical Systems, vol. 1, n°1 , pp. 403-412.
[10] Arsie I., Di Iorio S., Pianese C., Rizzo G., Sorrentino M., 2008, Recurrent Neural Networks for Air-Fuel Ratio Estimation and Control in Spark-Ignited Engines, Proceedings of the 17th IFAC World Congress, Seoul, July 6-11, pp. 1-8, ISBN: 9783902661005, DOI: 10.3182/20080706-5-KR-1001.3048.
[11] Nørgaard M., Ravn O., Poulsen N.L., Hansen L.K., Neural Networks for Modelling and Control of Dynamic Systems, 2000, Springer-Verlag, 1st ed., London.
[12] Patterson D.W., Artificial Neural Networks – Theory and Applications, 1995, Prentice Hall, Inc., Englewood Cliffs, New Jersey.
[13] Arsie I., Pianese C., Sorrentino M., 2006, A procedure to enhance identification of recurrent neural networks for simulating air-fuel ratio dynamics in SI engines, Engineering Applications of Artificial Intelligence, vol. 19, no°1, pp. 65-77.
[14] Larminie J., Dicks A., Fuel Cell Systems Explained, 2002, Wiley, New York.
[15] Montgomery D.C., Design and Analysis of Experiments, 2001, John Wiley and Sons, Inc., 5th Edition, New York.
[16] GENIUS Generic diagnosis instrument for SOFC systems, EU project n. 245128, 2010.